



Brief Communication: Limitations of Medical X-ray Computed Tomography for Estimating Ice Content in Permafrost Samples

Mahya Roustaei¹, Jonas Darey², Zakieh Mohammadi³, Daniel Fortier^{2, 4}

5 ¹ UGent Geotechnical Institute, Ghent University, Technologiepark 68, 9052 Zwijnaarde, Belgium

² University of Montreal, Department of Geography, Montreal, Canada

³ WSP Canada Inc., Calgary, Canada

⁴ Centre for Northern Studies, Laval University, Quebec, Canada

10 *Correspondence to:* Mahya Roustaei (Mahya.Roustaei@UGent.be)

Abstract. X-ray Computed tomography (CT) is increasingly used to estimate ice contents in permafrost samples. In this study, CT-derived estimates of volumetric ice content obtained from medical CT scans were compared with laboratory measurements for 261 samples from northern Canada (Nunavut and Yukon). The results showed that medical CT systematically underestimated ice in sediment-rich and organic-poor samples, and overestimated it in ice-rich, organic-rich samples. Agreement improved only when ice contents exceeded ~75% and organic matter was low. Errors arose from unresolved pore ice, organic matter misclassified as ice, and threshold sensitivity. Given these limitations, along with the associated cost and processing effort, we conclude that medical CT is better suited for visualizing cryostructures and heterogeneity than for routine quantification of ice content. By contrast, higher-resolution industrial CT can provide more accurate quantification of ice contents in suitable samples.

Key words: Permafrost; Ground ice; Volumetric ice content; X-ray computed tomography (CT); Pore ice.



1 Introduction

Quantifying ground ice is fundamental for understanding permafrost stability and predicting thaw-related ground deformation (Hjort et al., 2022; Mohammadi and Hayley, 2023). Historically, descriptive systems by Pihlainen and Johnston (1963) and Linell and Kaplar (1966) have been widely adopted in geotechnical applications in North America. These methods rely on visual assessments and ice characteristics are described by terms such as hardness (e.g., hard or soft), structure (e.g., clear, porous, or stratified), and colour. Over the years, these two descriptive approaches have proven to be unreliable, inconsistent, and sometimes misleading, being too general to precisely describe permafrost cryostructures. French and Shur (2010) proposed an alternative and more precise way to describe permafrost where cryostructures associated with excess ice content can be rapidly identified. Yet, it is a visual description which results can be difficult to reproduce among people with varied experience of permafrost description. These visual logs are typically supplemented by a limited number of laboratory measurements, in which volumetric ice content is determined from mass and volume measured in the frozen state and after oven-drying to constant mass. Despite its simplicity, laboratory measurement is constrained by cost, time, and handling effort, and it is destructive. As a result, spatial coverage is limited and repeat measurements on the same specimen are not possible.

Computed tomography (CT) has been proposed as a non-destructive alternative, providing detailed visualization of permafrost samples and offering the potential for quantitative estimation of ice, sediment, and gas fractions (Calmels and Allard, 2004, 2008; Dillon et al., 2008; Fortier et al., 2012; Lapalme et al., 2017; Fan et al., 2021; Roustaei et al., 2025). However, translating CT imaging into reliable estimates of soil components is not straightforward.

CT images are composed of voxels, which are 3D pixels formed by stacking 2D slices with specific spacing. Each voxel has an in-plane resolution defining the x–y dimensions, while the slice spacing defines the third dimension. The CT resolution sets its detection limit, with features needing to be at least twice the voxel size to be detected (Capowiez et al., 1998). When a voxel contains more than one component, their densities are averaged, producing the partial volume effect (Capowiez et al., 1998), which complicates quantitative analysis and leads to errors in volume estimation. (Roustaei et al., 2025). In the case of permafrost soils, pore ice within fine-grained samples is commonly unresolved at the resolution of medical CT scanners, leading to systematic underestimation of ice content. These errors are further compounded by density threshold segmentation, which often misclassifies materials such as ice, pore ice, and organic matter because of overlapping density range. Organic matter adds a level on complexity as it typically has a wide range of density due to its various states of decomposition from poorly decomposed fibrous peat to well-decomposed humified organic soils. As a result, volumetric ice content derived from medical CT scans might differ substantially from laboratory values.

This study presents a comparison of CT-derived and laboratory-measured ice contents was conducted for 261 permafrost samples collected in the Canadian Arctic. The analysis focuses on assessing the suitability of medical CT for quantifying volumetric ice content and on identifying the methodological challenges associated with resolution, partial volume effects, and segmentation approaches. A special attention is given to the impact of organic matter content on the volumetric ice content estimates using CT.



2 Methods and Materials

2.1 Sample provenance

Permafrost cores were collected on Bylot Island, Nunavut under ADAPT program and during field campaigns in 2016 and 2019 at representative wet and mesic sites (73°09' N, 80°00' W; 73°08' N, 79°58' W). Additional cores were collected in 2015
60 near Beaver Creek, Yukon (62°24' N, 140°52' W). Cores extracted using a portable core-drill, and were sealed, labelled, and kept below 0 °C from field to laboratory until analysis.

2.2 CT scanning and image processing

The same samples were scanned at Institut National de la Recherche Scientifique (INRS), Quebec City, using a commercial medical CT scanner (Siemens SOMATOM Sensation 64) with voxel resolutions of 0.18–0.24 mm in the x–y plane and 0.4–
65 0.6 mm in the z direction. CT scan images were processed in Dragonfly (Version 2020.2) to isolate the samples and remove external elements such as the stage, bags, and air. Regions of interest (ROIs) were defined using a classifier trained on 30 ADAPT project samples. Ice, sediment, and gas were segmented using published Hounsfield Unit (HU) ranges (gas: –1024 to –321, ice: –320 to 560, sediment: 561 to 3071) (Calmels and Allard, 2004; Calmels et al., 2010; Taina et al., 2008). Organic matter was not segmented directly due to its variable density, which often caused misclassification as ice or sediment.

70 2.3 Laboratory measurements

Volumetric ice content was derived from measurements of sample mass and volume in the frozen and oven-dried states, using gravimetric water content and frozen bulk density. Sample volume was obtained using the water displacement method, whereby the volume of liquid displaced by an immersed vacuum-sealed sample in a plastic bag is measured, providing an accurate estimate of bulk volume even for irregularly shaped specimens. Measurements were obtained for 261 samples, with
75 organic matter content determined for a subset of 81 samples. Organic matter content was determined for a subset of 81 samples using the loss on ignition (LOI) method: samples were oven-dried at 105 °C, combusted at 550 °C for 4 h, and the mass loss attributed to organic matter. Based on the measured values, the samples were classified into three groups: < 10 %, 10–20 %, and > 20 % organic matter. The dataset, including laboratory and CT-derived volumetric ice contents, is available on Zenodo (<https://doi.org/10.5281/zenodo.17451138>) (Fortier et al., 2025).

80



3 Results

3.1 Comparison of CT and laboratory values

To evaluate the performance of medical CT scans for quantifying ice, laboratory measurements of ice content (V_{Lab}^{ice}) were compared with CT-derived estimates (V_{CT}^{ice}) across all 261 samples. Figure 1 summarizes these comparisons. CT estimates were positively correlated with laboratory values but diverged systematically from the 1:1 line (Figure 1a). Residuals ($\Delta V_{ice} = V_{Lab}^{ice} - V_{CT}^{ice}$) showed a mean bias of -12.9% and a root mean squared deviation of 25.6% . Underestimation exceeded 60% at the low end of the V_{Lab}^{ice} range, while overestimation reached about 30% in ice-rich, organic-rich samples (Figure 1b).

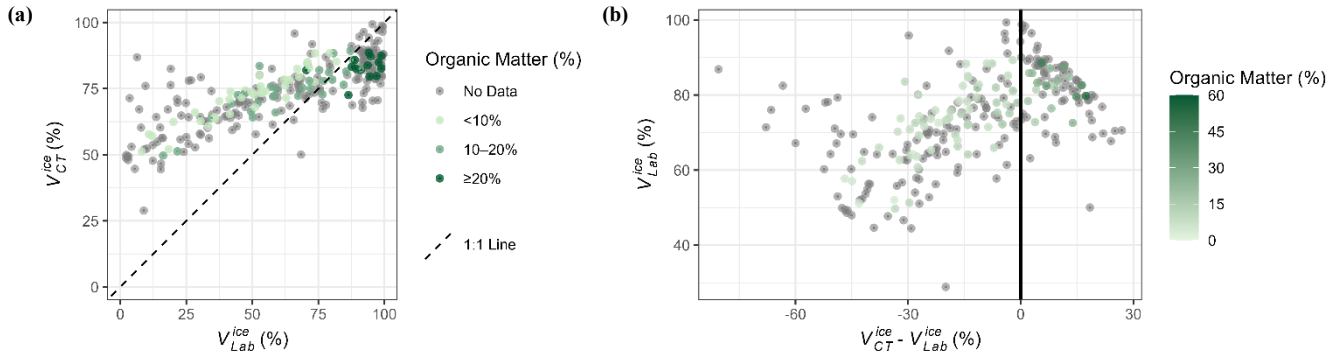


Figure 1. (a) Lab-measured (V_{Lab}^{ice}) vs. CT-estimated (V_{CT}^{ice}) volumetric ice content. Divergence from the 1:1 line shows bias. Results show systematic underestimation of V_{ice} for ice poor samples, shifting toward systematic overestimation for ice rich samples (b) Residuals ($\Delta V_{ice} = V_{Lab}^{ice} - V_{CT}^{ice}$) plotted against lab-measured volumetric ice content.

Figure 1b shows that residuals were strongly dependent on sample composition. For $V_{Lab}^{ice} < 75\%$, residuals were predominantly negative, indicating systematic underestimation. For $V_{Lab}^{ice} \geq 75\%$, residuals were smaller and more symmetrically distributed about zero, although both underestimation and overestimation occurred. In the subset with organic matter (OM) data, low-OM samples ($0-10\%$), which in this dataset generally coincide with lower ice contents, consistently showed negative residuals. In contrast, higher-OM samples displayed positive residuals, with the largest positive bias observed in the $\geq 20\%$ OM class. Overall, volumetric ice content was underestimated in all low-OM samples and overestimated in nearly all high-OM samples.

3.2 Sensitivity of CT estimates to HU threshold selection

This study also assessed the sensitivity of CT-derived ice content estimates to Hounsfield Unit (HU) thresholds. Previous work has applied widely varying thresholds for ice segmentation, resulting in inconsistent outcomes. To examine this effect, published thresholds were applied to two representative samples. As shown in Table 1, estimated ice volumes varied substantially, from strong underestimation to marked overestimation relative to laboratory values. Sample 1 from Bylot Island exhibited a broad density range (-1024 to 3071 HU), whereas Sample 2 from Beaver Creek showed a narrower range (-1024



to 2847 HU). Figure 2 illustrates segmentation of a region of interest from Sample 1, where ice is highlighted in blue using the –320 to 560 HU threshold. These results demonstrate that CT-based estimates are highly sensitive to threshold selection, which restricts their reproducibility for volumetric ice quantification.

110 **Table 1. Volumetric ice content of two representative samples estimated using HU thresholds from this study and previous literature, with laboratory measurements shown for reference.**

Study / Source	ID (Figure 2)	HU Thresholds (Low–High)	Volumetric Ice Content	
			Sample 1	Sample 2
Laboratory (reference)	—	—	817,77	380,95
This study	A	–320 to 560	524,60	251,12
Kawamura (1988)	B	~–50 to –40	513,80	268,35
Dillon et al. (2008)	C	–864 ^(a) to –241 ^(a)	27,71	8,21
Calmels et al. (2010)	D	–150 to –40	27,14	20,28
Crabeck et al. (2016)	E	–74 ^(b)	209,11	77,30
Lapalme et al. (2017)	F	–320 to 750	2,36	1,03
Lieb-Lappen et al. (2017)	G	~–464 ^(a, c) to 1071 ^(a, c)	554,74	324,52
Wendy (2025)	H	–170 to –83	624,49	368,98

Notes:
(a) Converted from gray levels
(b) For pure ice
(c) For sea ice

115

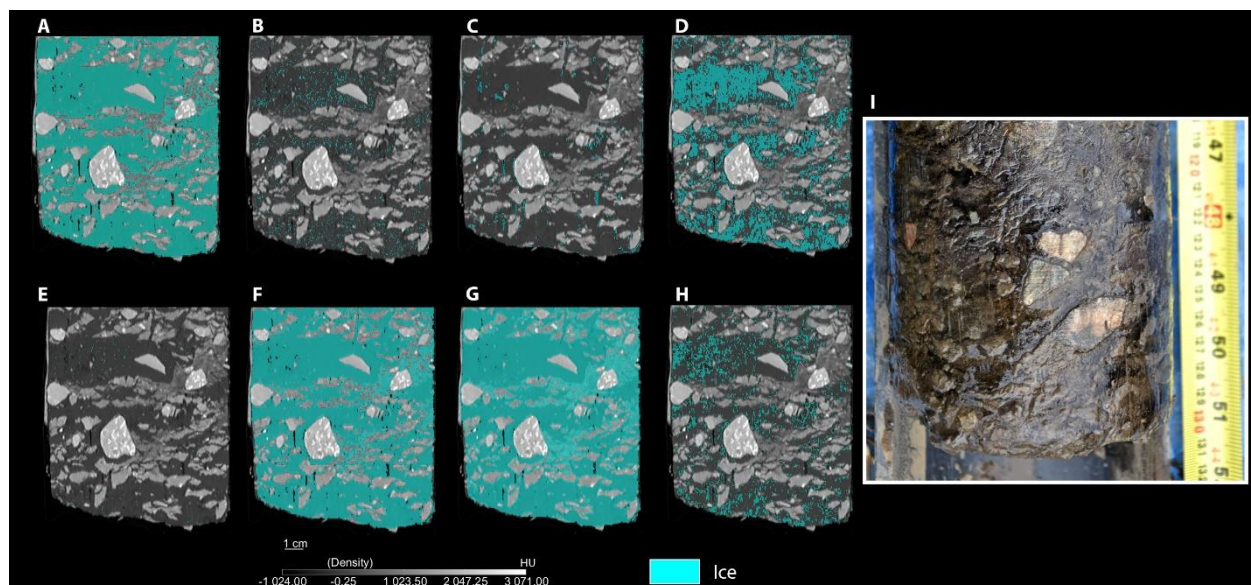


Figure 2. Comparison of ice volumes estimated for Sample 1 using the density thresholds from this study (A) and those reported in the literature (B–H), corresponding to study IDs in Table 1. Panel I shows a photograph of the sample, consisting of suspended sandy silt and gravel within an ice matrix.

4 Discussion and outlook

This study highlights the main key limitations of commercial medical CT for estimating volumetric ice content of permafrost samples. Scans of 261 permafrost cores clearly demonstrate that medical CT systematically misestimates volumetric ice content, with discrepancies strongly linked to sample composition. This limitation is largely results from the mismatch between scanner resolution and the characteristic pore-ice-organic structure of permafrost materials. At the resolution of medical CT, which is much coarser than sediment porosity, pore ice typically occupies volumes smaller than a voxel, and mixed voxels record averaged density values that fall outside the ice range. These partial-volume artifacts lead to systematic underestimation when the sediment fraction is high (Capowiez et al., 1998; Clausnitzer and Hopmans, 2000; ; Calmels et al., 2010). Organic matter adds further complications. In organic-rich samples, positive residuals arise from the overlap in density between organic matter and ice. Portions of the organic fraction fall within the HU range assigned to ice and are therefore misclassified, producing overestimation (Calmels et al., 2010; Roustaei et al., 2025). This effect was most pronounced in samples with $\geq 20\%$ organic matter.

Threshold selection introduces an additional source of error. Published HU ranges vary widely, and applying different thresholds to the same samples in this study produced results that ranged from severe underestimation to substantial overestimation relative to laboratory values. Even when thresholds are calibrated against reference data, unresolved pore ice, organic matter misclassification, and the partial-volume effect introduce uncertainties that limit the transferability of correction factors (Lapalme et al., 2017).



Together, these findings show that systematic underestimation in ice-poor samples, overestimation in organic-rich samples, and sensitivity to HU thresholds all stem from CT imaging artifacts. As a result, empirical corrections may reduce error within a single dataset but cannot overcome the fundamental limitations imposed by CT resolution and material density overlap.

140 While medical CT cannot be recommended as a routine method for quantifying volumetric ice content, it remains valuable for identifying cryostructures and characterising sample heterogeneity, providing essential qualitative insight into the internal structure of frozen cores.

5 Code and data availability

The dataset used in this study, including laboratory-derived volumetric ice contents, CT-derived volumetric compositions, and
145 associated metadata, is available at Zenodo (<https://doi.org/10.5281/zenodo.17451138>) (Fortier et al., 2025). Image processing workflows were performed in Dragonfly (Version 2020.2). No custom code was developed beyond standard segmentation and regression analysis.

6 Author contributions.

DF contributed to conceptualization of the study. JD, MR, ZM carried out data curation. JD, MR, ZM performed the formal
150 analysis and data processing. JD conducted the laboratory and CT analyses and supported the overall investigation. DF, JD contributed to methodology development, including creation of the classifier in Dragonfly. DF was responsible for funding acquisition. DF, MR provided supervision and guidance. MZ conducted validation of results. MZ prepared the original draft, and all authors contributed to writing, review, and editing of the manuscript.

7 Competing interests

155 At least one of the (co-)authors is a member of the editorial board of The Cryosphere.

8 Acknowledgment

We thank Elisabeth Hardy-Lachance for providing permafrost samples from Bylot Island, Nunavut and Michel Sliger for his help in the laboratory to measure volumetric water content of permafrost samples.

9 Financial support

160 This project was supported by the National Sciences and Engineering Research Council of Canada Discovery Grant to Daniel Fortier.



10 References

- Calmels, F., Allard, M., 2008. Segregated ice structures in various heaved permafrost landforms through CT Scan. *Earth Surf Processes Landf* 33, 209–225. <https://doi.org/10.1002/esp.1538>
- 165 Calmels, F., Allard, M., 2004. Ice segregation and gas distribution in permafrost using tomodesitometric analysis. *Permafrost & Periglacial* 15, 367–378. <https://doi.org/10.1002/ppp.508>
- Calmels, F., Clavano, W., Froese, D., 2010. Progress On X-ray Computed Tomography (CT) Scanning In Permafrost Studies, in: *In Proceedings of the 6th Canadian Conference On Permafrost. Presented at the 63rd Canadian Geotechnical Conference & 6th Canadian Permafrost Conference, Calgary, AB, Canada*, pp. 1353–1358.
- 170 Capowicz, Y., Pierret, A., Daniel, O., Monestiez, P., Kretschmar, A., 1998. 3D skeleton reconstructions of natural earthworm burrow systems using CAT scan images of soil cores. *Biology and Fertility of Soils* 27, 51–59. <https://doi.org/10.1007/s003740050399>
- Clausnitzer, V., Hopmans, J.W., 2000. Pore-scale measurements of solute breakthrough using microfocus X-ray computed tomography. *Water Resources Research* 36, 2067–2079. <https://doi.org/10.1029/2000WR900076>
- 175 Crabeck, O., Galley, R., Delille, B., Else, B., Geilfus, N.-X., Lemes, M., Des Roches, M., Francus, P., Tison, J.-L., Rysgaard, S., 2016. Imaging air volume fraction in sea ice using non-destructive X-ray tomography. *The Cryosphere* 10, 1125–1145. <https://doi.org/10.5194/tc-10-1125-2016>
- Dillon, M., Fortier, D., Kanevskiy, M., Shur, Y., 2008. Tomodesitometric analysis of basal ice, in: *NICOP 2008. Presented at the The 9th International Conference on Permafrost, University of Alaska Fairbanks, Fairbanks, Alaska, USA*, pp. 361–366. <https://doi.org/10.13140/2.1.2043.5526>
- 180 Fan, X., Lin, Z., Gao, Z., Meng, X., Niu, F., Luo, J., Yin, G., Zhou, F., Lan, A., 2021. Cryostructures and ground ice content in ice-rich permafrost area of the Qinghai-Tibet Plateau with Computed Tomography Scanning. *J. Mt. Sci.* 18, 1208–1221. <https://doi.org/10.1007/s11629-020-6197-x>
- Fortier, D., Kanevskiy, M., Shur, Y., Stephani, E., Dillon, M., 2012. Cryostructures of Basal Glacier Ice as an Object of Permafrost Study: Observations from the Matanuska Glacier, Alaska, in: *Proceedings of 10th International Conference on Permafrost. Unpublished, Salekhard, Russia*, pp. 107–112. <https://doi.org/10.13140/2.1.4876.2569>
- 185 Fortier, D., Mohammadi, Z., Roustaei, M., Darey, J., 2025. Dataset supporting “Limitations of Medical X-ray Computed Tomography for Estimating Ice Content in Permafrost Samples.” <https://doi.org/10.5281/zenodo.17451138>
- French, H.M., Shur, Y., 2010. The principles of cryostratigraphy. *Earth Sciences review* 101, 190–206.
- 190 Hjort, J., Streletskiy, D., Doré, G., Wu, Q., Bjella, K., Luoto, M., 2022. Impacts of permafrost degradation on infrastructure. *Nat Rev Earth Environ* 3, 24–38. <https://doi.org/10.1038/s43017-021-00247-8>
- Kawamura, T., 1988. Observations of the internal structure of sea ice by X ray computed tomography. *J. Geophys. Res.* 93, 2343–2350. <https://doi.org/10.1029/JC093iC03p02343>



- 195 Lapalme, C.M., Lacelle, D., Pollard, W., Fortier, D., Davila, A., McKay, C.P., 2017. Cryostratigraphy and the Sublimation
Unconformity in Permafrost from an Ultraxerous Environment, University Valley, McMurdo Dry Valleys of
Antarctica. *Permafrost & Periglacial* 28, 649–662. <https://doi.org/10.1002/ppp.1948>
- Lieb-Lappen, R.M., Golden, E.J., Obbard, R.W., 2017. Metrics for interpreting the microstructure of sea ice using X-ray micro-
computed tomography. *Cold Regions Science and Technology* 138, 24–35.
<https://doi.org/10.1016/j.coldregions.2017.03.001>
- 200 Linell, K., Kaplar, C.W., 1966. Description and classification of frozen soils, in: *Permafrost International Conference*.
Presented at the 1st International Conference on Permafrost, West Lafayette, USA, pp. 481–487. Mohammadi, Z.,
Hayley, J.L., 2023. Qualitative evaluation of thaw settlement potential in permafrost regions of Canada. *Cold Regions
Science and Technology* 216, 104005. <https://doi.org/10.1016/j.coldregions.2023.104005>
- 205 Pihlainen, J.A., Johnston, G., 1963. Guide to a field description of permafrost for engineering purposes. National Research
Council of Canada. <https://doi.org/10.4224/40003252>
- Roustaei, M., Pumple, J., Harvey, J., Froese, D., 2024. Ground ice estimation in permafrost samples using industrial Computed
Tomography. *The Cryosphere*, 19, 4259–4275, 2025, <https://doi.org/10.5194/tc-19-4259-2025>
- Taina, I.A., Heck, R.J., Elliot, T.R., 2008. Application of X-ray computed tomography to soil science: A literature review.
Can. J. Soil. Sci. 88, 1–19.
- 210 Wendy. 2025. Processing Script for Cryostratigraphy Using X-ray Computed Tomography Scans of Permafrost Cores.
Available at: [https://www.mathworks.com/matlabcentral/fileexchange/33010-processing-script-for-cryostratigraphy-
using-x-ray-computed-tomography-scans-of-permafrost-cores?utm_source=chatgpt.com](https://www.mathworks.com/matlabcentral/fileexchange/33010-processing-script-for-cryostratigraphy-using-x-ray-computed-tomography-scans-of-permafrost-cores?utm_source=chatgpt.com) (Accessed: October 24,
2025).